Contributed paper

OPTO-ELECTRONICS REVIEW **11**(3), 203–209 (2003)

Improvement methods of reconstruction process in digital holography

S. PAŚKO* and R. JÓ WICKI

Institute of Micromechanics and Photonics, Warsaw University of Technology
8 Boboli Str., 02-525 Warsaw, Poland

Problems of quality improvement in holographic images and a reconstruction time reduction are discussed. The convolution and Fresnel approaches are presented. For both methods the algorithm improvement is proposed. Basing on a special transmittance function calculation, a computation time significantly decreases. For the Fresnel approximation, an autocorrelation factor from the reconstructed image is removed. The presented ideas are illustrated by exemplary images for each step of computation. Advantages and disadvantages of the methods are discussed.

Keywords: digital holography, convolution approach, response function, image filtration.

1. Introduction

Simplicity of the registration process, no wet processing and the possibility of immediate reprocessing of stored data are the main reasons of continuously increasing interest in digital holography (DH). The data are stored in a mass-digital memory and they can be used in any place equipped with a computer working in a communication network. Assuming the number of CCD matrix pixels to be 1024×1024, one hologram without any compression is registered using one MB file. Therefore, a commercially available hard disk may accommodate many thousands of holograms. The objects registered can be located in not easily accessible areas, and the object registration can be accomplished fully automatically. The data could be distributed simultaneously to other computers to estimate various object features.

Digital recording of holograms by a CCD camera is correct as long as the sampling theorem is fulfilled. This means that every interferometric fringe of the hologram has to be sampled at least by two pixels of the CCD matrix. Therefore the angle between the object and reference waves must be sufficiently small. In practice, the above condition implies registration of small objects or objects located sufficiently far from the hologram plane. These restrictions do not allow for some applications of digital holography in multimedia techniques. However, a rapid progress observed in the semiconductor technology permits to express optimistic forecasts for near, or even further future.

The reconstruction process in DH is fully digital and no optic arrangement is needed. All computer calculations can be performed basing on the Rayleigh-Sommerfeld (R-S) diffraction formula [1]. However, using this formula directly results in time consuming procedures. It is better to use its simplified versions reducing to Fresnel approximation or convolution approaches [2]. In the majority of applications, the first method is more popular due to its fast calculations. Unfortunately, variable pixel dimension at the hologram plane and the noise introduced by the zero-diffraction order represent main disadvantageous features of the Fresnel approximation method [3]. In the paper, some image improvements are considered reducing the noise sources in the holographic image. Subtracting the average value of the holographic intensity distribution from the holographic fringe image to eliminate the zero-order diffraction beam is the simplest and fastest method to improve the image quality [3]. The successive subtraction of intensity distributions registered, separately, by the object and reference beams is similar method to the one mentioned above but it can be effective under the stable experimental conditions [4]. Inserting, adequately, a mask into the image spectrum, low spatial frequencies including the zero diffraction order can be eliminated. The mask transmittance should be a continuous function to avoid undesirable diffraction intensity oscillations in the holographic image [5]. The suppression of the conjugate image is a more complex operation. Locating a diaphragm between the object being registered and the hologram plane is one of the solutions [6]. First, during the reconstruction procedure, the field distribution at the diaphragm plane is determined. This field, truncated by a virtual diaphragm of proper dimensions, allows finding the field distribution at the hologram plane. It is used at the final stage to determine the image field distribution. Such an approach suppresses the higher spatial frequencies of the object and removes the conjugate image. The convolution approach gives the image with constant pixel dimensions [2]. However, due to the limited reconstructed image area and more complex algorithm, with comparison to the Fresnel approximation method inducing time-consuming procedures, this ap-

*e-mail: s.pasko@mchtr.pw.edu.pl

proach is applied less frequently. In the paper, a method decreasing the calculation time is proposed.

2. Method of noise reduction in the central part of holographic images

Subtracting the average value of the intensity distribution from the holographic fringe image, the zero-order diffraction beam is removed. Afterwards, using Fourier transformation of the remaining intensity distribution the spectrum is received. It is presented in Fig. 1(a) in a pictorial manner, and in Fig. 1(b) for a laboratory realised hologram.

Black central part in Fig. 1(b) results from the above mentioned subtractive pre-processing. However, three components real image, conjugate image, and a residuum from zero-order diffraction beam are present. The boundaries between the constitutive areas are never precisely well defined. Therefore it is difficult to elaborate an automatic program to separate the area of the demanded real image.

We propose to make use of a symmetry property of the auto-correlation component with respect to the spectrum centre.

Let $h(x,y)$ be the intensity distribution at the hologram plane after subtracting its average value. Fourier transform $u(m,n)$ of the intensity $h(x,y)$ described by the following equation

$$u(m,n) = FFT^{-1}[h(x,y)], \qquad (1)$$

is a base to improve the holographic image quality. In general, the quantities m, n are the coordinates in the Fourier domain of the hologram intensity distribution, moreover, they have not be treated as physical parameters. It is worth emphasizing that in the case of Fourier hologram with an object situated at infinity these quantities take the role of angular coordinates.

For the every spectrum column m, the centre of the intensity distribution and its shift with respect to the spectrum centre are determined by the following relation

$$n_G = \frac{\sum_N u(m,n)n}{\sum_N u(m,n)}, \qquad (2)$$

where N is the number of the samples in the every column.

The distribution of the gravity centre vs. the column number, calculated for an exemplary object, is presented in Fig. 2.

Choosing a level value of $|n_G - N_0|$ denoting by δ in Fig. 2 where $N_0 = N_0/2$, the columns with the gravity centres below the chosen level are removed, what is described in mathematical form by the following equation

$$\forall m \in \langle 0, M| \wedge \left(|n_G - N_0| < \delta\right) \Rightarrow u(m,n) = 0, \qquad (3)$$

In consequence, majority of the spectrum related to the auto-correlation component is removed and the procedure result is presented in Fig. 3(a). The result received for laboratory hologram is shown in Fig. 3(b).

Some non-zero columns, visible in the central part of Fig. 3(b) have no significant influence on the image quality due to the low spatial frequency filtration. In the next step, the conjugate image area is removed putting zero for all columns located at the conjugate image side, what is presented in Figs. 4(a) and 4(b).

From the observer point of view it is more convenient to displace the spectrum gravity centre denoted by n_c and m_c, where

$$m_C = \frac{\sum_N \sum_M u(m,n)m}{\sum_N \sum_M u(m,n)}, \quad n_C = \frac{\sum_N \sum_M u(m,n)m}{\sum_N \sum_M u(m,n)}, \qquad (4)$$

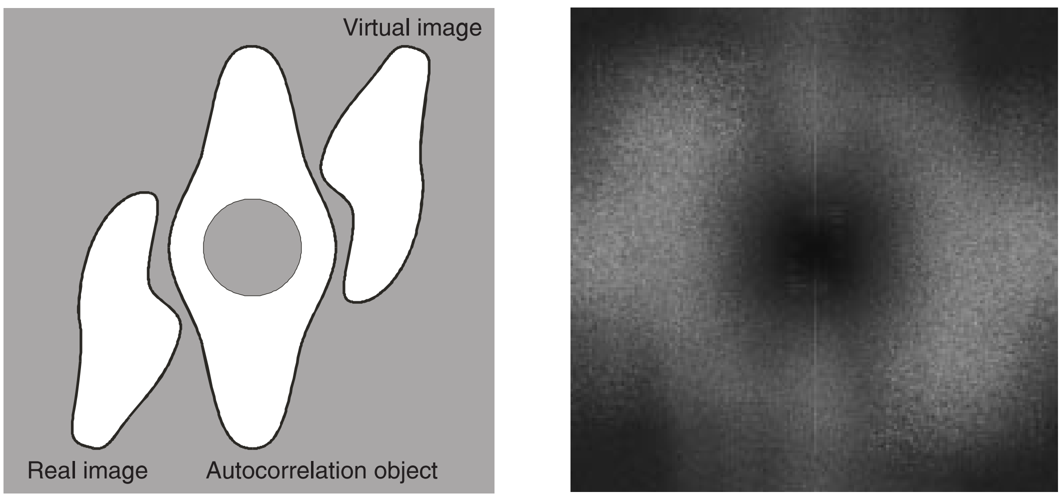

(a) (b)

Fig. 1. Spatial spectrum of a typical hologram. Pictorial (a) and real (b) cases.

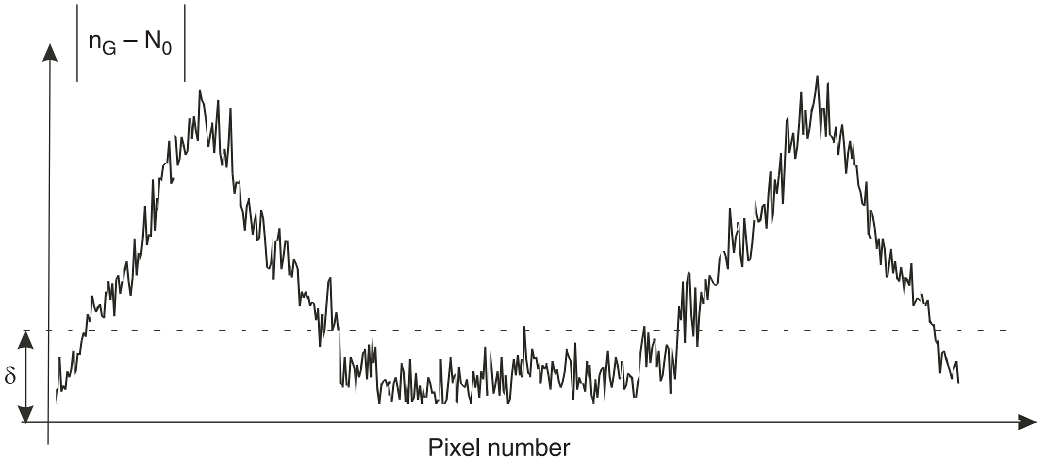

Fig. 2. Gravity centre distribution for a chosen object.

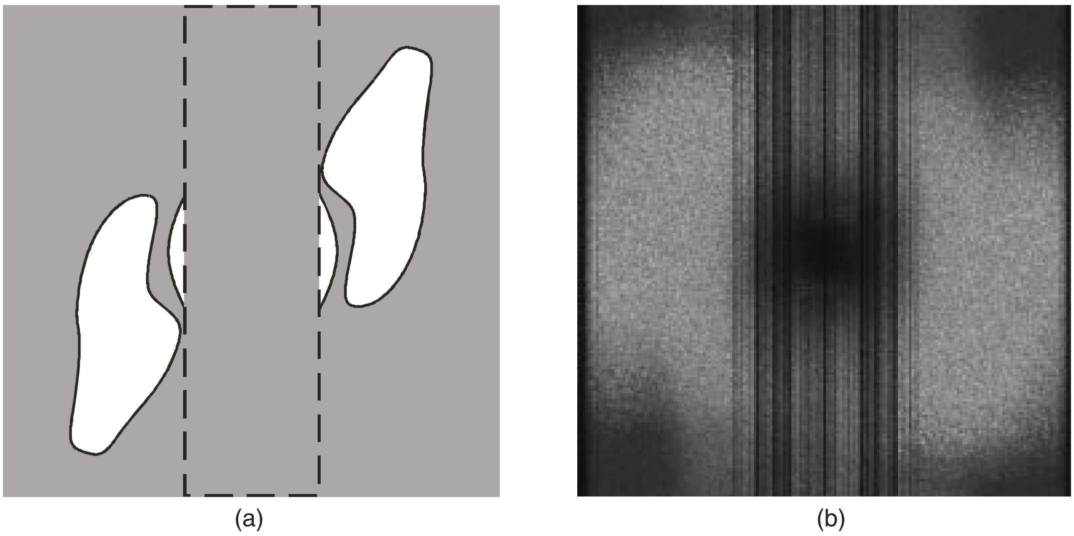

Fig. 3. Spatial spectrum after zero-order beam filtration. Pictorial (a) and real (b) cases.

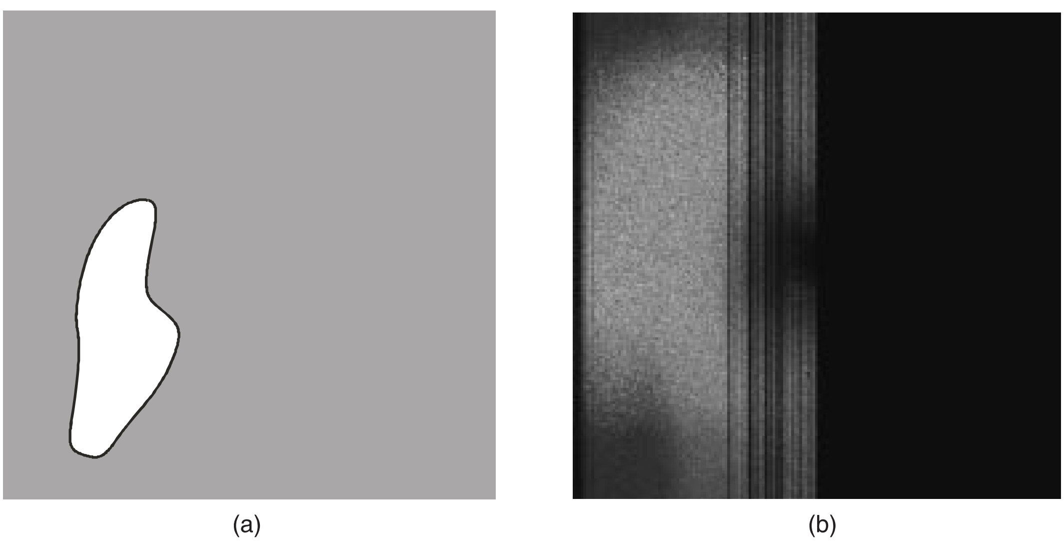

Fig. 4. Spatial spectrum after filtrating the zero-order beam and the conjugate image area.

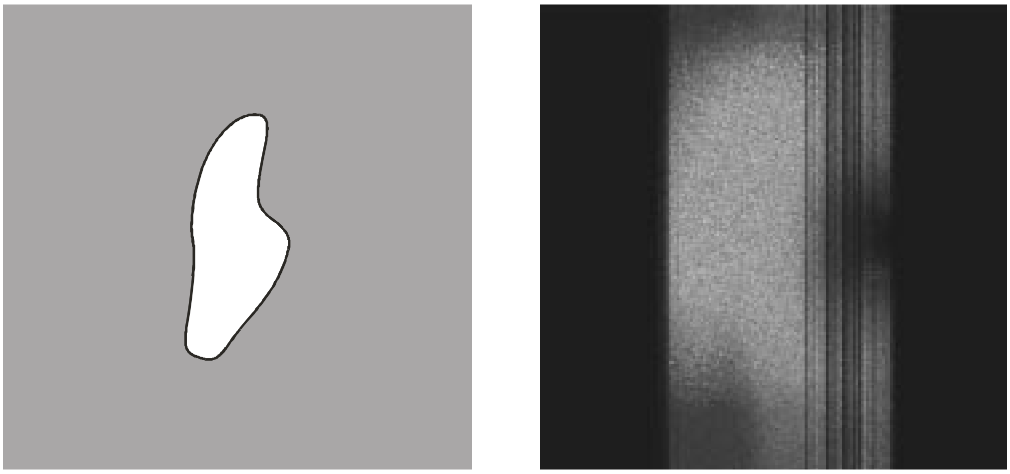

(a) (b)

Fig. 5. Spectrum centring. Pictorial (a) and real (b) cases.

to the image centre. The new image is given by u'

$$u'(m,n) = u(m - m_C, n - n_C). \tag{5}$$

The result of mentioned operation is presented in Figs. 5(a) and 5(b) for the pictorial and real cases, respectively.

Finally the inverse Fourier transformation

$$h'(x, y) = FFT^{-1}[u'(m,n)], \tag{6}$$

is applied to receive the complex distribution $h'(x,y)$ at the hologram plane with reduced noises. This distribution is a base to calculate a reconstructed image [7].

To show the method effectiveness, two holographic image reconstructions from the same hologram were accomplished. First image, Fig. 6(a), was obtained by removing a constant component from the hologram intensity. A distinct noise can be seen around the image of the object registered. Applying the method described above, the image becomes free of noises [Fig. 6(b)].

3. Convolution approach – performance improvement

As it was mentioned above, the convolution approach is one of the basic methods of digital hologram reconstruction. In a simplified version, it can be described by following expression

$$b' = FFT^{-1}\{FFT\{h \cdot r\}FFT\{g\}\}, \tag{7}$$

where

$$g(m,n) = \frac{\exp\left\{\frac{2i\pi}{\lambda}\sqrt{d'^2 + (m - M/2)^2 \Delta\xi^2 + (n - N/2)^2 \Delta\eta^2}\right\}}{\sqrt{d'^2 + (m - M/2)^2 \Delta\xi^2 + (n - N/2)^2 \Delta\eta^2}}, \tag{8}$$

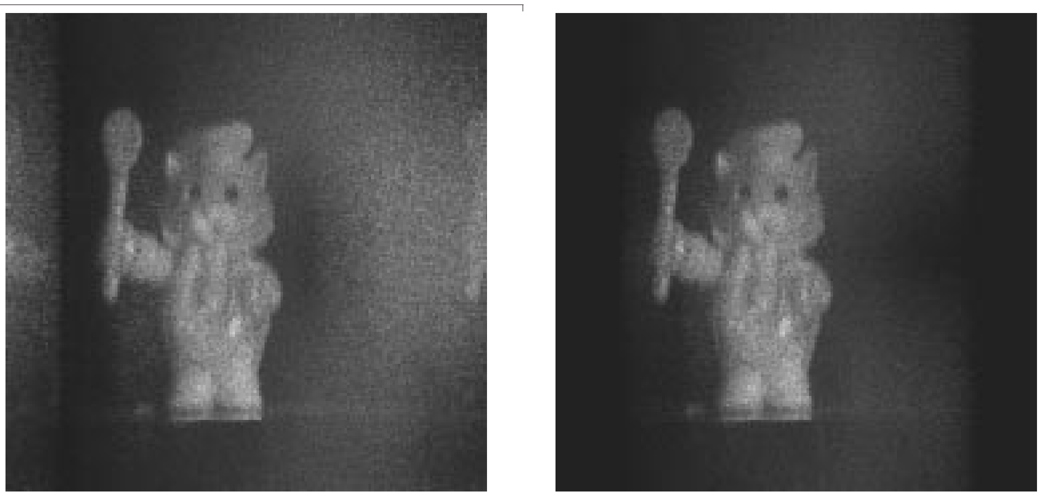

(a) (b)

Fig. 6. Reconstructed images before (a) and after proposed filtration (b).

h and *r* represent the intensity and wave front distribution at the hologram plane, respectively [2]. Kreis in Ref. 2 has proposed a modification of this method. The Fourier transform of $g(m,n)$ was substituted by $G(m',n')$, the analytically calculated Fourier transform of $g(m,n)$, i.e.,

$$b' = FFT^{-1}\{FFT\{h \cdot r\} \cdot G\}, \tag{9}$$

where

$$G(m,n) = \exp\left\{\frac{2\pi i d'}{\lambda}\sqrt{1 - \frac{\lambda^2\left(m + \frac{M^2 \Delta\xi^2}{2d'\lambda}\right)}{M^2 \Delta\xi^2} - \frac{\lambda^2\left(n + \frac{N^2 \Delta\eta^2}{2d'\lambda}\right)}{N^2 \Delta\eta^2}}\right\}. \tag{10}$$

It is the easiest approach to find the $G(m,n)$ term but it requires square root and exponential function for each pixel calculation. These mathematical operations require relatively a lot of time of the co-processor. Because during the computation three Fourier transforms are used, the convolution approach is much slower than the Fresnel approximation approach. On the other hand it offers the reconstructed image usually free of the zero order beam. The zero order appears in the image when a number of pixels is very high and the angle between the object and reference beams is small enough. Another interesting feature of the method is the pixel size constancy in the reconstructed images. The pixel size in this case is independent of the holographic arrangement parameters and is equal to the size of CCD pixel. This feature causes also some inconvenience, because during the reconstruction process only a fragment of the registered object which corresponds to the size of CCD matrix, is restored. In order to obtain a whole image, one has to compose it from several sub-images calculated during sequential reconstruction processes.

The image obtained suffers from the existence of discontinuity located at place of sub-images connection. This fault can lead to errors especially when the phase for holographic interferometry is calculated. In order to avoid these errors, it is proposed to stretch the size of hologram artificially for example from 1024×1024 to 2048×2048, for instance, by adding zeros around the original image. In result, the reconstruction of a real object area of size 2048×2048 times the CCD pixel size is obtained. Unfortunately, calculations in this case need a lot of time due to increasing the object size so, quicker algorithms are badly needed. Considering a formula given by Eq. (7) it is possible to increase the speed of image calculation, for instance by introducing hardware *FFT* calculation or by modifying the function $g(m,n)$, representing the impulse response of the optical arrangement.

3.1. New algorithm

Our aim is to propose the solution to improve the reconstruction using the convolution method with less time required. At the beginning, let us assume that the aperture of the CCD camera has a rectangular shape and it is possible to represent it by a superposition of two infinite longitudinal apertures, perpendicular to each other. The transfer function of the infinite longitudinal aperture is the same for each perpendicular cross-section. The impulse response of such an aperture can be calculated for one cross-section only and duplicated for the other ones. Because there are two perpendicular apertures considered, the same operation must be repeated for the other one. Procedures needed to obtain full information about the transfer function are presented below together with the figures illustrating their performance.

Generally, the calculation process can be divided into three parts. First, the pulse response function of single lines in both directions must be computed. They are given by

$$g_m(m) = \frac{1}{i\lambda}\frac{\exp\left\{\frac{2i\pi}{\lambda}\sqrt{d'^2 + (m - M/2)^2 \Delta\xi^2}\right\}}{\sqrt{d'^2 + (m - M/2)^2 \Delta\xi^2}}, \tag{11}$$

$$g_n(n) = \frac{1}{i\lambda}\frac{\exp\left\{\frac{2i\pi}{\lambda}\sqrt{d'^2 + (n - N/2)^2 \Delta\eta^2}\right\}}{\sqrt{d'^2 + (n - N/2)^2 \Delta\eta^2}}. \tag{12}$$

Next the Fourier transform is calculated. In consequence, one-dimensional spectrum of the response function is obtained (see Fig. 7)

$$G(m') = FFT(g_m(m)), G(n') = FFT(g_n(n)). \tag{13}$$

In following, the results of 1D operation are stretched to 2D ones by duplicating the lines (Fig. 8). Two separate data blocks are created in which the results for "*x*" and "*y*" direction, respectively, are stored

$$G_1(m',n') = G(m'), \; G_2(m',n') = G(n'). \tag{14}$$

Last operation can be named as the final composition (Fig. 9). It consists of 2D multiplication of G_1 and G_2. Be-

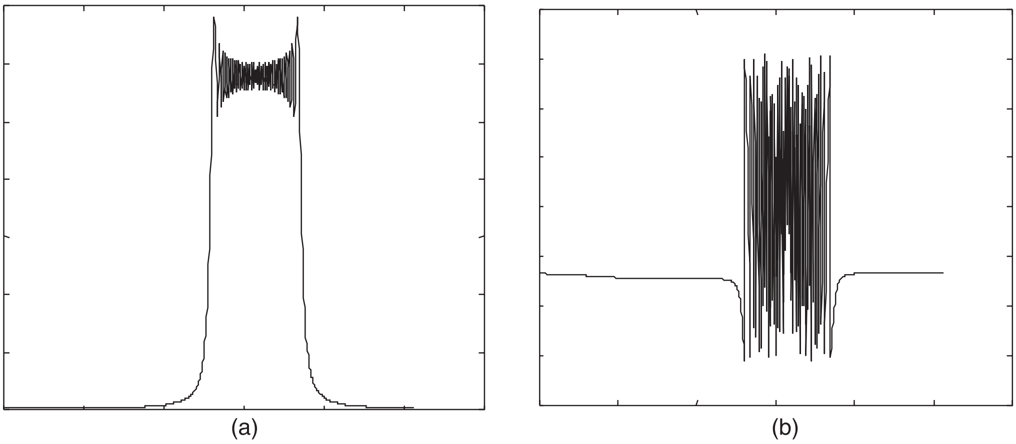

Fig. 7. Image of one line $G(k')$: (a) intensity and (b) phase.

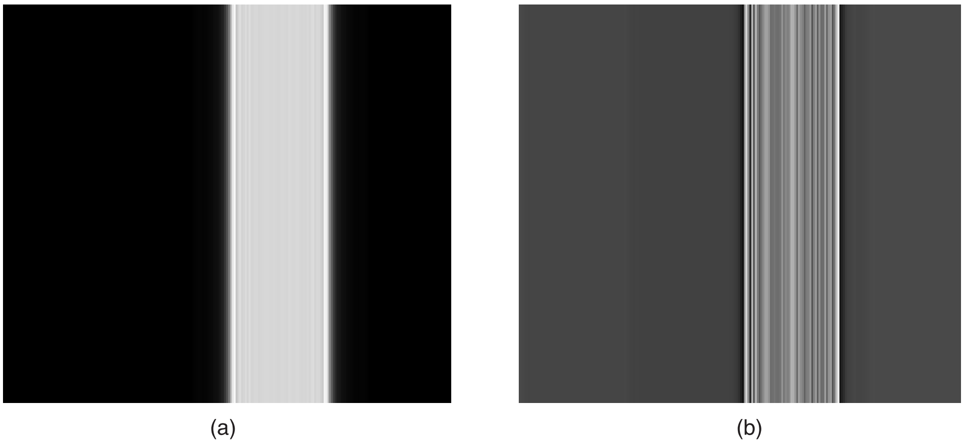

Fig. 8. View after duplicating the lines of G: (a) intensity and (b) phase.

cause G_2 represents the data along the "y" axis, therefore in the multiplication conjugated values of G_2 must be used

$$G(m',n') = \prod_{m=1}^{M} \prod_{n=1}^{N} G_1(m',n') conj(G_2(m',n')). \quad (15)$$

The algorithm presented is approximately four times faster than the algorithm proposed by Kreis. This feature results from reducing the number of called procedures calculating square root and exponential. In consequence, the number of floating point operations is six times smaller. However, larger number of processor operations due to the array transfer limits the speed of computation. Maximum error in the intensity reconstruction introduced by this approach is approximately 1%.

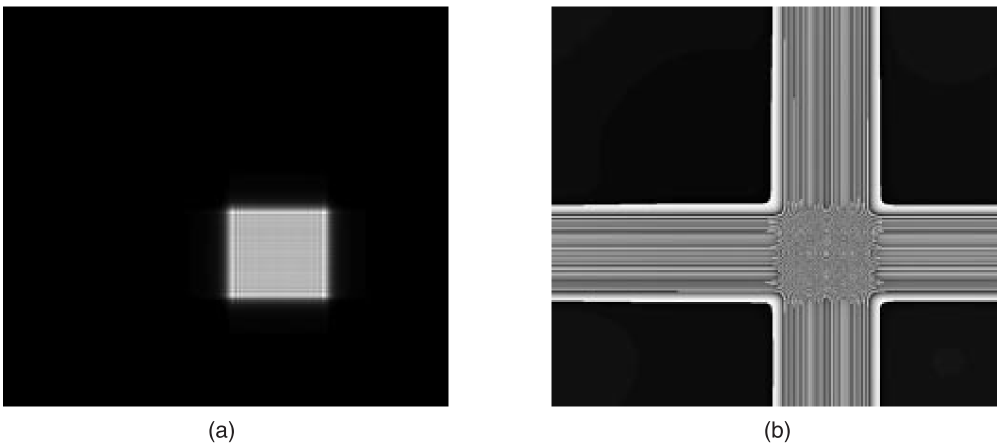

Fig. 9. Fourier transform $G(k',l')$ of the impulse response $g(k,l)$: (a) intensity and (b) phase.

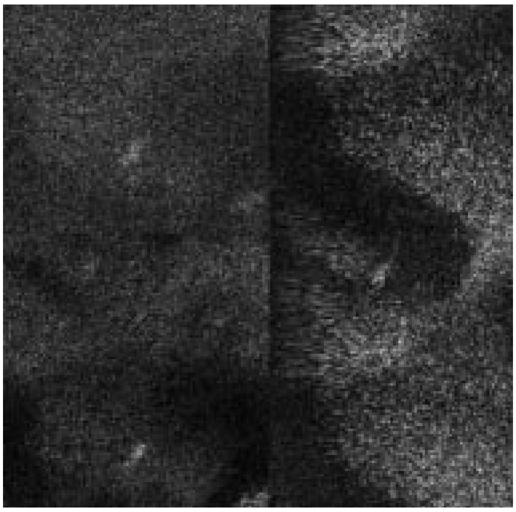

Fig. 10. Reconstructed image of a screw composed of 4 subimages.

Fig. 11. Image of a screw reconstructed by a modified procedure.

3.2. Direct image reconstruction

Having the algorithm with increased speed one may consider to improve the process of full image reconstruction using the convolution method. The conventional technique requires forming the image from sub-images obtained upon reconstruction with shifted co-ordinates in Eq.(8). The result of this procedure is often unsatisfactory due to significant errors at the borders of sub-images, as shown in Fig. 10. We propose to apply the method which relies on artificial enlargement of size of hologram. In our case, its original size of 1024 by 1024 pixels was changed to 2048 by 2048. It gave the possibility to reconstruct the area that was four times larger and covered the whole image domain. A restored image is free of disturbances encountered in the previous case as shown in Fig. 11. One essential disadvantage of this approach is its big memory requirement. If there are not enough memory resources, the computer starts procedure of data swapping with hard disc. The swapping process can slow down the computer considerably and the calculation lasts then very long.

4. Conclusions

Digital holography will become an attractive method to record and transform the images for multimedia techniques in future. Clear, noiseless images transformed in real time are main requirements not fulfilled yet. The methods proposed in the paper are aiming at achieving this goal but the results received are far from moderate expectations yet. The availability of the CCD camera with high resolving power is one of the most important factors facilitate the aim.

Acknowledgements

This work was supported by the State Committee for Scientific Research under the project 8T07D04621.

References

1. L.P. Jarosławski and N.S. Merzljakow, “Methods of digital holography”, *Consultants Bureau*, New York, 1980.
2. T. Kreis and W. Jupner, “Principles of digital holography”, *Proc. Fringe* **97**, 353–363 (1997).
3. T. Kreis and W. Jupner, “Suppression of dc term in digital holography”, *Opt. Eng.* **36**, 2357–2360 (1997).
4. S. Seebacher, W. Osten, and W. Juptner, “Measuring shape and deformation of small objects using digital holography”, *Proc. SPIE* **3479**, 104–115 (1998).
5. E. Cuche, P. Marquet, and C. Depeursinge, “Spatial filtering for zero-order and twin-image elimination in digital off-axis holography”, *Appl. Optics* **39**, 4070–4075 (2000).
6. G. Pedrini, P. Froning, H. Fessler, and HJ. Tiziani, “In-line digital holographic interferometry”, *Appl. Optics* **37**, 6262–6269 (1998).
7. S. Paśko and R. Jóźwicki, “Novel Fourier approach to digital holography”, *Opto-Electron. Rev.* **10**, 89–95 (2002).